Published in final edited form as:
Acta Biomater. 2011 September ; 7(9): 3404–3411. doi:10.1016/j.actbio.2011.05.010.

Submicron–sized UHMWPE wear particle analysis from revised SB Charité III total disc replacements

Ilona M. Punt[1,*], **Ryan M. Baxter**[2,*], **André van Ooij**[3], **Paul C. Willems**[1], **Lodewijk W. van Rhijn**[1], **Steven M. Kurtz**[2,4], and **Marla J. Steinbeck**[2]

[1] Maastricht University Medical Center, Maastricht, the Netherlands [2] Drexel University, Philadelphia, PA, USA [3] Viecuri Medical Center, Venlo, the Netherlands [4] Exponent Inc., Philadelphia, PA, USA

Abstract

Submicron-sized particles are frequently observed in retrieved total hip and knee periprosthetic tissues and appear to be critical in the activation of the phagocytic inflammatory response. In this paper, the concentration, size and shape of ultra-high molecular weight polyethylene (UHMWPE) wear particles between 0.05–2.00 μm were determined after isolation from periprosthetic tissues from retrieved lumbar SB Charité III total disc replacements (TDR) using scanning electron microscopy (SEM). For comparison, UHMWPE wear particles were isolated from gamma-air sterilized total hip arthroplasty (THA) revision tissues. The mean concentration of UHMWPE particles in TDR tissues was 1.6×10^9/gram of tissue (range 1.3–2.0), which was significantly lower than the concentration of 2.3×10^9/gram of THA revision tissue (range 1.8–3.2) (p=0.03). The mean particle size (equivalent circular diameter, TDR: 0.46 μm, THA: 0.53 μm, p=0.60) and mean shape were comparable between TDR and THA (aspect ratio, TDR: 1.89, THA: 1.99, p=0.35; roundness, TDR: 0.58, THA: 0.56, p=0.35). However, the TDR particles in general were smaller and more round. Although no correlations were found between visible damage to the UHMWPE core and the concentration or shape of the UHMWPE particles, a positive correlation was found between increasing particle size and increasing rim penetration of the TDR core (p=0.04). The presence of UHMWPE particles of similar size and shape in TDR tissue albeit lower in concentration might explain why unlike THA, pain rather than osteolysis is the major reason for revision surgery.

Keywords

polyethylene; wear; total disc replacement; scanning electron microscopy; UHMWPE

Contact information corresponding author: IM Punt, Department of Orthopaedic Surgery, Maastricht University Medical Center, P. Debyelaan 25, P.O. Box 5800, 6202 AZ Maastricht, the Netherlands, Telephone: +31 43 3871317, Fax: +31 43 3874893, i.punt@mumc.nl.
*Both authors contributed equally to this work.

Introduction

For patients who suffer from degenerative disc disease, lumbar fusion of the affected vertebral segment has been the standard treatment of care. However, studies have shown that fusion of a single level results in an accelerated rate of degeneration in adjacent discs and vertebral levels due to altered biomechanics [1, 2]. Alternatively, total disc replacement (TDR) achieves both a resolution of pain and preserves the motion segment of the functional spine unit, and thus, represents an appealing surgical alternative [3, 4]. The SB Charité III (Link/De Puy, Germany/USA), the first FDA-approved TDR device in the U.S., includes an ultra-high molecular weight polyethylene (UHMWPE) core articulating between two cobalt chromium (CoCr) endplates [5]. Currently, the short- and mid-term clinical results of the Charité TDR are at least equivalent to the clinical outcomes of lumbar interbody fusion, with a success rate of 65.2% and 57.8% at two and five years follow-up, respectively [3, 6–8]. Nevertheless, as several studies have identified a low quality of evidence supporting the efficiency of TDR over fusion, the long-term effectiveness of this relatively new medical device compared to lumbar fusion remains unclear [9–11].

During the development of TDR component technology, a combination of biomaterials and design concepts were adopted from devices used in total hip arthroplasty (THA) and total knee arthroplasty (TKA). However, based on previous clinical experience with THA and TKA, the accumulation of UHMWPE wear debris is implicated in the development of inflammatory reactions that contribute to osteolysis and aseptic implant loosening [12–17]. The extent of this inflammatory response is affected by several characteristics of the UHMWPE wear debris, which include particle concentration (number per gram of tissue), size and shape [18–21]. Smaller particles tend to be the most biologically active, this was also true for elongated particles compared to a round-like or spherical particle shape [17, 18, 22].

While osteolysis and loosening represent the most frequent reason for revision surgery of THA and TKA implants [23–27], the development of osteolysis around TDRs is rarely observed [28–32]. Initially, it was thought that the generation of substantial amounts of UHMWPE wear debris in the spine was unlikely due to a limited range of motion and the absence of a synovial joint [5, 30]. These views were based on an *in vitro* study of Serhan et al. [30], showing only minimal wear debris generation after 10 million cycles. However, in a recent immunohistological study, we identified the concomitant presence of UHMWPE particles (≥2.05 μm), phagocytic cells and pro-inflammatory cytokines in periprosthetic tissues around retrieved TDRs [33]. The study was limited by the inability of polarized light microscopy to quantify the full range of submicron-sized UHMWPE particles. Therefore, the aims of the present study were to determine the concentration, size and shape of UHMWPE wear particles between 0.05–2.00 μm in periprosthetic tissues from retrieved TDRs, to compare these findings with wear debris isolated from THA revision tissues, and to identify correlations between the characteristics of TDR wear debris and visible damage to the UHMWPE core.

We hypothesize that UHMWPE wear debris generation from TDR implants should be minimal and if generated the characteristics of the particles should differ from THA implant results. To determine if these hypotheses are true, we isolated and characterized wear debris from TDR and THA revision tissues.

Materials and Methods

Implant characteristics

In total 34 SB Charité III TDRs of 29 patients were collected during revision surgery at the Maastricht University Medical Center. In a previous study, 16 available patient tissues were evaluated for the presence of inflammation and >2.05 μm UHMWPE particles [33]. Of these, we selected tissues from five single-level TDRs (male = 2, female = 3) implanted with non-coated SB Charité III design manufactured by LINK to evaluate the size, shape and number of <2 μm UHMWPE particles using scanning electron microscopy. The surface damage of the corresponding UHMWPE implant components was also evaluated. The five patients included in the present study showed similar clinical variables and tissue responses as the other 11 TDR cases that were reported in the previous study (Table 1) [33]. Periprosthetic fibrous tissue samples were obtained from random locations relative to the implant at the time of revision surgery. Revision of these five patients was indicated after 9 years (range 6–12 years) due to persistent back and leg pain (Table 2). The mean age of the patients at the time of primary surgery was 37 years (range 33–46 years). Separately, UHMWPE particles were evaluated in tissue samples from the single TDR revised for osteolysis. Since the development of osteolysis around TDRs is rarely observed, we separately compared this case to the control THAs revised for osteolysis (detailed below).

Periprosthetic tissues were obtained from the Maastricht Pathology Tissue Collection (MPTC). Collection, storage and use of tissue and patient data were performed in agreement with the “Code for proper secondary use of human tissue in the Netherlands” (http://www.fmwv.nl). All procedures were performed in accordance with Institutional Review Board (IRB) guidelines of Drexel University.

Controls

The TDR tissue samples were compared with periprosthetic fibrous tissue from five revised metal-on-UHMWPE THAs, which were revised after 13 years (range 11–15 years) due to wear and/or osteolysis (Table 2). These controls were chosen for comparison based on the gamma-air sterilized UHMWPE core material used in these devices as well as the SB Charité III design. The control THA group had comparable gender distribution and the patients were of similar age at implantation (p=1.00 and p=0.05, respectively) as the TDR group. However, due to the extended longevity of THA implants, the implantation time was significantly longer in the THA group compared to TDR (p=0.02) (Table 2).

Tissue digestion protocol

The tissue samples were fixed in 10% phosphate buffered formalin and the bone tissue was subsequently decalcified. During decalcification, the specimens were kept in a 3.5% sodium formate and 25% formic acid solution [34], until they were soft enough and could be embedded in paraffin. Particle isolation and characterization was performed using methods modified from Margevicius et al. [15]. Using polarized light microscopy, several areas of the fibrous tissue that were thought to be representative of tissue containing UHMWPE particles were removed from the paraffin block. This tissue was deparaffinized in 10 ml xylene overnight at room temperature and washed twice in xylene and twice in 100% ethanol for three minutes each. After drying for two hours at room temperature, 0.02–0.03 grams of tissue were placed in a polypropylene tube and digested in 5 ml 65% HNO_3 at room temperature for 24 hours. After the first 24 hours, the tubes were agitated and left to digest for an additional 24 hours.

Following digestion, the solutions containing UHMWPE wear debris were thoroughly mixed with a G560 vortex (Scientific Industries, Bohemia, NY) for three 30-second

intervals. Finally, the tubes were placed in an ultrasonic bath (Cole-Parmer, Vernon Hills, Illinois) for two minutes to achieve uniform particle dispersion. Subsequently, the sample was vacuum-filtered through a polycarbonate membrane with a pore size of 1.0 μm (Whatman, Billerica, MA) and the filtrate containing submicron particles was collected and saved. After filtration, the membrane was washed with 10 ml of fresh 65% HNO_3, which was added to the membrane surface for 10 minutes and subsequently pulled through by a vacuum. Finally, using a separate side-arm flask, this washing process was repeated with methanol. To prevent particle agglomeration, the filtrate containing submicron particles was diluted with 15 ml of dH_20 containing 2% Nonidet P-40® (NP40 substitute) (AppliChem GmbH, Darmstadt, Germany), a non-ionic surfactant. The solution containing surfactant was mixed with a vortex for three 30-second intervals, and subsequently placed in an ultrasonic bath for two minutes to achieve uniform particle dispersion and to further reduce agglomeration. After sonication, samples were immediately filtered through a membrane with a pore size of 0.05 μm. As with the first membrane, the second polycarbonate membrane was sequentially washed with 10 ml solutions of 65% HNO_3 followed by methanol, which were again collected in separate sidearm flasks. Based on the thorough digestion of small quantities of tissue, centrifugation steps were not employed during particle isolation; however, this may require modification for larger tissue samples. Each membrane was then dried for 2 hours at room temperature, and prepared for scanning electron microscopy.

Scanning electron microscopy (SEM)

Polycarbonate membranes with isolated UHMWPE wear debris were fixed onto aluminum stubs with double-sided carbon tape, and sputter coated with a 5-nm-thick layer of platinum/palladium using a 208 HR vacuum sputter coater (Cressington, Watford, England). This method of sample preparation was necessary to eliminate sample drift and/or damage by the electron beam at high magnifications. Coated samples were inserted into an XL30 environmental scanning electron microscope (SEM, FEI/Phillips, Hillsboro, OR) equipped with a Schottky field-emission gun and an energy dispersive x-ray detector (EDAX, Mahwah, NJ) to visualize UHMWPE wear debris. Imaging was performed at a working distance of 12 mm and a beam intensity of 5kV. All sample preparation and imaging were performed in the Drexel University Centralized Research Facilities.

After demonstrating a homogenous distribution of particles, polycarbonate membranes with a pore size of 1.0 μm were imaged at magnifications of 500X and 1,000X; five and 10 images were collected, respectively. Separately, polycarbonate membranes with a pore size of 0.05 μm were imaged at a magnification of 12,000X; 10 images were collected from each of three separate regions. Altogether, the membranes contained a minimum of 1000 particles in the size range of 50–2000 nm.

Particle analysis

Image analysis of SEM micrographs was initially performed using a gray-scale level threshold in Adobe Photoshop (San Jose, CA). Subsequently, using a scale bar from each micrograph, the individual particle areas and dimensions were determined using a custom macro in NIH ImageJ (National Institutes of Health, USA). The resulting areas and dimensions were used to characterize particle concentration, size (equivalent circular diameter) and shape (aspect ratio, roundness) based on guidelines for particle analysis outlined in ASTM F1877 (Table 3) [35].

Validations

To validate particle isolation techniques, two tissue samples (0.02–0.03 g) from primary spine surgery were selected. Control tissues were processed using the digestion and imaging methods as mentioned above.

To determine the effect of using a small tissue weight, 0.025- and 0.25-gram samples were processed using the digestion and imaging methods provided above. After image processing, particle concentrations were determined for each sample.

To validate methods for evaluating particle morphology, we obtained reference standard UHMWPE particles (RM8385), which were generated by rubbing a gamma-irradiated UHMWPE pin against a textured surface in a reciprocating pin-on-disk system (National Institute of Standards & Technology (NIST), Gaithersburg, MD). A solution containing UHMWPE particles with a nominal diameter of 7 μm was vacuum-filtered through a polycarbonate membrane with a pore size of 1 μm. Particles were analyzed using imaging and image processing methods described above and the obtained values of particle size were then compared to values provided in the reference standard. The mean difference (± sem) in the percentage of particles was 1.3% (± 0.4) across all size ranges (Fig. 1).

Visible UHMWPE damage

The wear patterns of each retrieved polyethylene core was analyzed at the rim and dome. Dome and rim penetration measurements were performed in these five cores using a calibrated digital micrometer (± 0.001 mm accuracy) [36, 37].

Statistical analysis

Sample-size analyses were performed using the THA control samples; a two-fold decrease in particle concentration was detected at a power of 80% and a level of significance at 0.05. Analyses were performed using SPSS 16.0. To evaluate differences between TDR and THA Mann-Whitney U tests were used. Relationships between surface damage and the characteristics of the submicron UHMWPE particles were analyzed using Spearman rho correlation. Significance was assumed at p values less than 0.05.

Results

To determine UHMWPE particle concentrations, we isolated and characterized wear debris in periprosthetic tissues from five TDR and five THA revision cases. Over a billion wear particles per gram of tissue were present in all five TDR patient samples. The mean TDR UHMWPE particle concentration was 1.6×10^9/gram (range 1.3 – 2.0). Although present, the amount was significantly lower than the concentration of particles in THA periprosthetic tissues (2.3×10^9/gram, range 1.8 – 3.2) (p=0.03, power=0.6) (Table 4). For the separately evaluated TDR case revised for osteolysis, an elevated concentration of UHMWPE particles (2.6×10^9/gram of tissue) was detected that resembled the THA osteolytic revision concentrations.

Comparing particle size, no differences were observed between the mean equivalent circular diameter for TDR and THA particles (p=0.60). The mean equivalent circular diameter was 0.464 ± 0.050 μm and 0.529 ± 0.055 μm for TDRs and THAs, respectively. Although the overall particle size was similar for both groups, significantly more TDR particles were observed in the 50–200 nm size range (p=0.04), whereas particles in the 800–1000 and 1000–1250 nm size range were more frequent in THA tissues (p=0.03, p=0.01, respectively). For both groups, the highest frequency of particles was within in the 50–200 nm size range.

Analysis of UHMWPE wear particles from TDR and THA revision tissues revealed a wide range of particle shapes (Fig. 2A–D). Overall, no differences were observed for the mean particle aspect ratio between the two groups (p=0.35); TDR 1.890 ± 0.044 and THA 1.987 ± 0.070. Although the mean aspect ratio was similar for both groups, differences were observed in the individual aspect ratio ranges. For TDRs, particles with an aspect ratio between 1.25–1.50 were more frequently observed (p=0.04), whereas THA particles were increased in the 2.5–2.75 range (p<0.05). For both groups, the particle aspect ratio distribution reached a peak at 1.25–1.50, which rapidly dropped off below 1.25 and declined gradually above 1.5.

For roundness, no differences were observed between TDR and THA particles (p=0.35). Overall, the mean particle roundness was 0.578 ± 0.011 and 0.564 ± 0.008 for TDR and THA, respectively. Similar to findings for equivalent circular diameter and aspect ratio, differences between TDR and THA particle roundness were only observed in individual ranges. Specifically, TDR particles were more frequently observed in the 0.75–0.80 range (p=0.02), and in general were less fibrillar; whereas THA particles were increased in the 0.35–0.40 range (p=0.01). For both groups, the particle roundness distributions reached a maximum at 0.60–0.65, which decline at a similar rate below 0.60 and above 0.65. Taken together, these findings suggest the particle size (Fig. 3A) and shape (Fig. 3B, 3C) tended to be smaller and more granular (round) for TDR as compared to THA particles.

In the assessment of surface damage on retrieved UHMWPE components, dome as well as rim penetration patterns showed large variations between patients (Table 5). Due to this variation, the only positive correlation between regional component damage and UHMWPE particle characteristics was an increase in particle size with increasing linear rim penetration (mm) (p=0.04).

Discussion

Based on clinical experience with UHMWPE bearings in THA and TKA studies, it is known that UHMWPE wear particles play a critical role in the inflammatory responses that contribute to the development of osteolysis and, ultimately, the need for revision surgery [12, 14–18]. However, in TDRs, where osteolysis is rarely observed, the inflammatory role of UHMWPE is uncertain, in part because the characteristics of TDR wear particles *in vivo* have not been clearly defined [33]. Therefore, the current study was performed using scanning electron microscopy to determine following: 1) the concentration, size and shape of UHMWPE wear particles between 0.05–2.00 μm in periprosthetic tissues from retrieved TDRs, 2) to compare these findings with wear debris isolated from THA revision tissues, and 3) to identify correlations between the characteristics of TDR wear debris and visible damage to the UHMWPE core.

There are some limitations in the current study. First, a subset of 5 patients with non-coated and single level TDR was selected from our previous study [33]. This selection was chosen to eliminate potential complications of adjacent level TDRs and wear debris generation from coated metal surfaces. Moreover, no differences were observed between clinical variables or tissue responses of these 5 patients as compared to the other 11 patients from our previous study. Second, although this is a representative subset of TDR revisions, the revised components exhibited variable amounts of surface damage. As component damage was not a factor in patient selection, the characteristics of the UHMWPE wear particles are inclusive of a wide range of TDR component failure modes. Third, a 0.05 μm polycarbonate filter was chosen based on the ESEM study by Scott et al. [38] showing that only a small percentage (2.8%) of THA particles were smaller than the 0.05 μm pore size [38]. Thus, it is unlikely that the method of sample preparation contributes to an under- or overestimate of the

concentration, size or shape of wear particles present in the current TDR and THA revision tissues. Fourth, the TDR and THR wear particles were obtained from UHMWPE that was gamma irradiated in air, a historical sterilization method that is no longer employed for spine and orthopedic implants. Nevertheless, the particle data reported here provide a crucial, and heretofore unavailable, reference point for future studies of conventional gamma inert sterilized UHMWPEs that are currently used for contemporary total disc arthroplasty.

The assumption that UHMWPE wear debris generation from TDRs implant would be minimal is not supported by our findings. The results from the present study showed an UHMWPE particle concentration of 1.6×10^9 particles/gram of tissue in the TDR group. For this reason, future studies shall require additional samples to achieve higher statistical power.

Although few studies have evaluated the presence of wear debris in TDR revision tissues, case studies of TDR component wear and our previous work highlight the potential for wear particle accumulation [31, 33]. In the present study, gamma air-sterilized TDR component revision tissues contained $1.3–2.0 \times 10^9$ particles/gram of tissue. The concentration of UHMWPE wear particles in gamma air-sterilized THA component tissues was more variable ($1.8–3.2 \times 10^9$ particles/gram of tissue), but consistent with previous reports [14, 39]. Of note, the implantation time was longer for THAs as compared to TDR, so it is unclear whether an equivalent concentration of particles would be generated if the device remained functional for a longer period of time.

For the single case of TDR osteolysis revised in our hospital, we noted an elevated concentration of UHMWPE particles (2.6×10^9/gram). Thus, based on studies showing an osteolytic threshold for wear debris in THA revision cases [40, 41], the presence of an elevated number of particles after only 6 years of implantation introduces the possibility of an osteolytic threshold in the spine. If a linear wear rate is assumed, and based on the similar calculated number of UHMWPE particles generated annually for TDR (0.182×10^9/gram/year) and THA (0.180×10^9/gram/year) (p=0.60), it is conceivable that if TDR implantations were extended, the number of particles would reach equivalent concentrations as those observed in THA osteolytic revision cases.

In our previous study, we evaluated the presence of UHMWPE wear particles > 2 μm in TDR revision tissues [33]. Fifteen of the 16 patients had polarized light detectable wear debris, which ranged from 3.8 to 15.9 μm in length. As an extension of the previous study, all 5 tissues selected for ESEM analysis contained predominantly submicron wear debris (0.05 to 2 μm), which are considered to be more biologically active. Similarly, all 5 THA revision tissues contained wear debris in this size range, and particle sizes of the THA UHMWPE particles (mean 0.53 μm) were comparable to previous studies [14, 17, 24, 42]. Taking into account the use of a 0.05 cutoff filter in the present study, the mean particle size range for the THA tissues (0.41 to 0.7μm) was also comparable to previous reports of mean values ranging from 0.38 to 0.78 μm [12, 14, 17, 39]. In addition, based on a particle size cutoff of 0.1 μm, Howling et al. [24] showed that >80% of particles from THA gamma air-sterilized liners were between 0.1–0.5 μm, which agrees with the value of approximately 80% observed for THAs in the current study [24].

In general, the morphology of UHMWPE particles from TDR tended to be more rounded as compared to THA particles. For both TDR and THA, particle morphologies were predominantly globular, with the mean values of aspect ratio from individual patients ranging from 1.8 to 2.2. Fibrillar particles were also observed in both groups, but to a lesser extent. These findings were consistent with the determination of aspect ratio from previous studies of gamma air-sterilized THA particles, for which the mean was typically between 1.6

and 2.3 [24, 39, 43]. For particle roundness, which was calculated based on the parameter definition specified by ASTM, mean values ranged from 0.54 to 0.60 for both TDR and THA. Numerically, the roundness parameter specified by ASTM is identical to the inverse of aspect ratio. Thus, the mean values of roundness in the current study were also consistent with previously published data, which ranged from 0.42 to 0.63 [24, 39, 43].

In THA, UHMWPE wear patterns involve micro-adhesion and -abrasion, whereas wear patterns in a TDR core involve combined wear damage mechanisms. Specifically, in the central TDR dome region adhesive/abrasive wear mechanisms were comparable to those of THA, whereas at the rim wear patterns included a combination of micro-adhesion and -abrasion, and fatigue which is similar to wear observed in TKA [44]. The surface damage of the UHMWPE core was not correlated to either particle concentration or shape. The current retrieved UHMWPE TDR cores showed large inter-individual differences in adhesive/abrasive wear patterns at both the dome and rim. Despite this variability, patients with a higher rim penetration showed a significant increase in mean wear particle size or equivalent circular diameters (p=0.04).

Traditionally, the presence of submicron UHMWPE wear debris is implicated in the activation of a biological cascade associated with the onset of osteolysis at the bone-implant interface and, ultimately, aseptic implant loosening [18, 24, 45]. This response involves a number of cell types and the subsequent release of various cytokines and factors (e.g. tumor necrosis factor-alpha (TNF-α), interleukin 1 (IL-1), interleukin 6 (IL-6), prostaglandin E2 (PGE_2)) that promote adverse biological responses and/or bone loss [16, 46, 47]. In addition to particle size, particle concentration and shape can affect the release of osteolytic cytokines [18, 43, 48, 49]. In tissues around TDRs, these cytokines may contribute, either additionally or in a dualistic manner, to the development of neuroinflammatory-induced pain, as an inflammatory response was observed in all 5 TDR patient tissues revised for pain [33]. Specifically, TNF-α, IL-1, IL-6 and PGE_2 can induce peripheral sensitization of sensory neurons or affect pain indirectly by recruiting immune cells and up-regulating the release of pain mediators in the affected area [50, 51]. Thus, the full repertoire of inflammatory responses to wear debris in the spine has not been established.

Conclusion

TDR revision tissues contained over a billion wear particles/gram, and although lower than THA tissue concentrations, this represents a substantial load within the spinal tissue. Moreover, despite differences in loading and kinematics between the lumbar spine and the hip joint, the mean wear particle size and shape were comparable between TDR and THA. Taken together, these findings for historical gamma air-sterilized UHMWPE implicate wear debris is an important factor contributing to the need for TDR revision surgery. In THA, wear debris initiates an inflammatory response that directly contributes to the development of osteolysis. It is therefore conceivable that the lower TDR particle concentrations may account for the infrequent observation of TDR revision surgery for osteolysis, but nonetheless initiate neuroinflammation. Additional work is necessary to understand the contribution of particle-induced inflammation in the development of pain in the spine.

Acknowledgments

Institutional support was received in part from the National Institutes of Health, AR 56264.

References

1. Eck JC, Humphreys SC, Hodges SD. Adjacent-segment degeneration after lumbar fusion: a review of clinical, biomechanical, and radiologic studies. American journal of orthopedics (Belle Mead, NJ). 1999 Jun; 28(6):336–40.
2. Etebar S, Cahill DW. Risk factors for adjacent-segment failure following lumbar fixation with rigid instrumentation for degenerative instability. Journal of neurosurgery. 1999 Apr; 90(2 Suppl):163–9. [PubMed: 10199244]
3. Blumenthal S, McAfee PC, Guyer RD, Hochschuler SH, Geisler FH, Holt RT, et al. A prospective, randomized, multicenter Food and Drug Administration investigational device exemptions study of lumbar total disc replacement with the CHARITE artificial disc versus lumbar fusion: part I: evaluation of clinical outcomes. Spine. 2005 Jul 15; 30(14):1565–75. discussion E387-91. [PubMed: 16025024]
4. Geisler FH. The CHARITE Artificial Disc: design history, FDA IDE study results, and surgical technique. Clinical neurosurgery. 2006; 53:223–8. [PubMed: 17380756]
5. Link HD. History, design and biomechanics of the LINK SB Charite artificial disc. Eur Spine J. 2002 Oct; 11(Suppl 2):S98–S105. [PubMed: 12384729]
6. David T. Long-term results of one-level lumbar arthroplasty: minimum 10-year follow-up of the CHARITE artificial disc in 106 patients. Spine. 2007 Mar 15; 32(6):661–6. [PubMed: 17413471]
7. Guyer RD, McAfee PC, Banco RJ, Bitan FD, Cappuccino A, Geisler FH, et al. Prospective, randomized, multicenter Food and Drug Administration investigational device exemption study of lumbar total disc replacement with the CHARITE artificial disc versus lumbar fusion: five-year follow-up. Spine J. 2009 May; 9(5):374–86. [PubMed: 18805066]
8. Lemaire JP, Carrier H, Sariali el H, Skalli W, Lavaste F. Clinical and radiological outcomes with the Charite artificial disc: a 10-year minimum follow-up. Journal of spinal disorders & techniques. 2005 Aug; 18(4):353–9. [PubMed: 16021017]
9. Putzier M, Funk JF, Schneider SV, Gross C, Tohtz SW, Khodadadyan-Klostermann C, et al. Charite total disc replacement--clinical and radiographical results after an average follow-up of 17 years. Eur Spine J. 2006 Feb; 15(2):183–95. [PubMed: 16254716]
10. van den Eerenbeemt KD, Ostelo RW, van Royen BJ, Peul WC, van Tulder MW. Total disc replacement surgery for symptomatic degenerative lumbar disc disease: a systematic review of the literature. Eur Spine J. 2010 Aug; 19(8):1262–80. [PubMed: 20508954]
11. Yajun W, Yue Z, Xiuxin H, Cui C. A meta-analysis of artificial total disc replacement versus fusion for lumbar degenerative disc disease. Eur Spine J. 2010 Aug; 19(8):1250–61. [PubMed: 20364392]
12. Campbell P, Ma S, Yeom B, McKellop H, Schmalzried TP, Amstutz HC. Isolation of predominantly submicron-sized UHMWPE wear particles from periprosthetic tissues. Journal of biomedical materials research. 1995 Jan; 29(1):127–31. [PubMed: 7713952]
13. Doorn PF, Campbell PA, Worrall J, Benya PD, McKellop HA, Amstutz HC. Metal wear particle characterization from metal on metal total hip replacements: transmission electron microscopy study of periprosthetic tissues and isolated particles. Journal of biomedical materials research. 1998 Oct; 42(1):103–11. [PubMed: 9740012]
14. Maloney WJ, Smith RL, Schmalzried TP, Chiba J, Huene D, Rubash H. Isolation and characterization of wear particles generated in patients who have had failure of a hip arthroplasty without cement. The Journal of bone and joint surgery. 1995 Sep; 77(9):1301–10. [PubMed: 7673277]
15. Margevicius KJ, Bauer TW, McMahon JT, Brown SA, Merritt K. Isolation and characterization of debris in membranes around total joint prostheses. J Bone Joint Surg Am. 1994 Nov; 76(11):1664–75. [PubMed: 7962027]
16. Revell PA. The combined role of wear particles, macrophages and lymphocytes in the loosening of total joint prostheses. Journal of the Royal Society, Interface/the Royal Society. 2008 Nov 6; 5(28):1263–78.

17. Shanbhag AS, Jacobs JJ, Glant TT, Gilbert JL, Black J, Galante JO. Composition and morphology of wear debris in failed uncemented total hip replacement. J Bone Joint Surg Br. 1994 Jan; 76(1): 60–7. [PubMed: 8300684]
18. Green TR, Fisher J, Stone M, Wroblewski BM, Ingham E. Polyethylene particles of a 'critical size' are necessary for the induction of cytokines by macrophages in vitro. Biomaterials. 1998 Dec; 19(24):2297–302. [PubMed: 9884043]
19. Greenfield EM, Bechtold J. What other biologic and mechanical factors might contribute to osteolysis? The Journal of the American Academy of Orthopaedic Surgeons. 2008; 16(Suppl 1):S56–62. [PubMed: 18612015]
20. Kadoya Y, Kobayashi A, Ohashi H. Wear and osteolysis in total joint replacements. Acta orthopaedica Scandinavica. 1998 Feb.278:1–16. [PubMed: 9524528]
21. Sabokbar A, Fujikawa Y, Murray DW, Athanasou NA. Radio-opaque agents in bone cement increase bone resorption. J Bone Joint Surg Br. 1997 Jan; 79(1):129–34. [PubMed: 9020461]
22. Fang, H-W.; Hsu, SM.; Sengers, JV. Ultra-High Molecular Weight Polyethylene Wear Particles Effects on Bioactivity. NIST; 2003. Special Publication 1002
23. Hirakawa K, Bauer TW, Stulberg BN, Wilde AH. Comparison and quantitation of wear debris of failed total hip and total knee arthroplasty. Journal of biomedical materials research. 1996 Jun; 31(2):257–63. [PubMed: 8731215]
24. Howling GI, Barnett PI, Tipper JL, Stone MH, Fisher J, Ingham E. Quantitative characterization of polyethylene debris isolated from periprosthetic tissue in early failure knee implants and early and late failure Charnley hip implants. Journal of biomedical materials research. 2001; 58(4):415–20. [PubMed: 11410900]
25. Mochida Y, Boehler M, Salzer M, Bauer TW. Debris from failed ceramic-on-ceramic and ceramic-on-polyethylene hip prostheses. Clinical orthopaedics and related research. 2001 Aug.(389):113–25. [PubMed: 11501799]
26. Schmalzried TP, Callaghan JJ. Wear in total hip and knee replacements. The Journal of bone and joint surgery. 1999 Jan; 81(1):115–36. [PubMed: 9973062]
27. Willert HG, Semlitsch M. Reactions of the articular capsule to wear products of artificial joint prostheses. Journal of biomedical materials research. 1977 Mar; 11(2):157–64. [PubMed: 140168]
28. Fraser RD, Ross ER, Lowery GL, Freeman BJ, Dolan M. AcroFlex design and results. Spine J. 2004 Nov-Dec; 4(6 Suppl):245S–51S. [PubMed: 15541673]
29. McAfee PC, Geisler FH, Saiedy SS, Moore SV, Regan JJ, Guyer RD, et al. Revisability of the CHARITE artificial disc replacement: analysis of 688 patients enrolled in the U.S. IDE study of the CHARITE Artificial Disc. Spine. 2006 May 15; 31(11):1217–26. [PubMed: 16688035]
30. Serhan HA, Dooris AP, Parsons ML, Ares PJ, Gabriel SM. In vitro wear assessment of the Charite Artificial Disc according to ASTM recommendations. Spine. 2006 Aug 1; 31(17):1900–10. [PubMed: 16924206]
31. van Ooij A, Kurtz SM, Stessels F, Noten H, van Rhijn L. Polyethylene wear debris and long-term clinical failure of the Charite disc prosthesis: a study of 4 patients. Spine. 2007 Jan 15; 32(2):223–9. [PubMed: 17224818]
32. Licina P, Thorpe PLPJ. Osteolysis and complications associated with artifical disc replacement. J Bone Joint Surg Br. 2004; 86-b:460–1.
33. Punt IM, Cleutjens JP, de Bruin T, Willems PC, Kurtz SM, van Rhijn LW, et al. Periprosthetic tissue reactions observed at revision of total intervertebral disc arthroplasty. Biomaterials. 2009 Apr; 30(11):2079–84. [PubMed: 19155064]
34. Kristensen HK. An improved method of decalcification. Stain technology. 1948 Jul; 23(3):151–4. [PubMed: 18867628]
35. F 1877–05e Standard Practice for Characterization of Particles. ASTM International; 2005.
36. Kurtz SM, MacDonald D, Ianuzzi A, van Ooij A, Isaza J, Ross ER, et al. The natural history of polyethylene oxidation in total disc replacement. Spine. 2009 Oct 15; 34(22):2369–77. [PubMed: 19789469]
37. Kurtz SM, Patwardhan A, MacDonald D, Ciccarelli L, van Ooij A, Lorenz M, et al. What is the correlation of in vivo wear and damage patterns with in vitro TDR motion response? Spine. 2008 Mar 1; 33(5):481–9. [PubMed: 18317190]

38. Scott M, Widding K, Jani S. Do current wear particle isolation procedures underestimate the number of particles generated by prosthetic bearing components? Wear. 2001:1213–7.
39. Kobayashi A, Bonfield W, Kadoya Y, Yamac T, Freeman MA, Scott G, et al. The size and shape of particulate polyethylene wear debris in total joint replacements. Proceedings of the Institution of Mechanical Engineers. 1997; 211(1):11–5.
40. Kobayashi A, Freeman MA, Bonfield W, Kadoya Y, Yamac T, Al-Saffar N, et al. Number of polyethylene particles and osteolysis in total joint replacements. A quantitative study using a tissue-digestion method. J Bone Joint Surg Br. 1997 Sep; 79(5):844–8. [PubMed: 9331048]
41. Orishimo KF, Claus AM, Sychterz CJ, Engh CA. Relationship between polyethylene wear and osteolysis in hips with a second-generation porous-coated cementless cup after seven years of follow-up. The Journal of bone and joint surgery. 2003 Jun; 85-A(6):1095–9. [PubMed: 12784009]
42. Tipper JL, Galvin AL, Williams S, McEwen HM, Stone MH, Ingham E, et al. Isolation and characterization of UHMWPE wear particles down to ten nanometers in size from in vitro hip and knee joint simulators. J Biomed Mater Res A. 2006 Sep 1; 78(3):473–80. [PubMed: 16721797]
43. Mabrey JD, Afsar-Keshmiri A, McClung GA 2nd, Pember MA 2nd, Wooldridge TM, Mauli Agrawal C. Comparison of UHMWPE particles in synovial fluid and tissues from failed THA. Journal of biomedical materials research. 2001; 58(2):196–202. [PubMed: 11241339]
44. Kurtz SM, van Ooij A, Ross R, de Waal Malefijt J, Peloza J, Ciccarelli L, et al. Polyethylene wear and rim fracture in total disc arthroplasty. Spine J. 2007 Jan-Feb; 7(1):12–21. [PubMed: 17197327]
45. Ingham E, Fisher J. The role of macrophages in osteolysis of total joint replacement. Biomaterials. 2005 Apr; 26(11):1271–86. [PubMed: 15475057]
46. Willert HG, Bertram H, Buchhorn GH. Osteolysis in alloarthroplasty of the hip. The role of ultra-high molecular weight polyethylene wear particles. Clinical orthopaedics and related research. 1990 Sep.(258):95–107. [PubMed: 2203577]
47. Agarwal S. Osteolysis - basic science, incidence and diagnosis. Current Orthopaedics. 2004; 18:220–31.
48. Purdue PE, Koulouvaris P, Potter HG, Nestor BJ, Sculco TP. The cellular and molecular biology of periprosthetic osteolysis. Clinical orthopaedics and related research. 2007 Jan.454:251–61. [PubMed: 16980902]
49. Yang SY, Ren W, Park Y, Sieving A, Hsu S, Nasser S, et al. Diverse cellular and apoptotic responses to variant shapes of UHMWPE particles in a murine model of inflammation. Biomaterials. 2002 Sep; 23(17):3535–43. [PubMed: 12109677]
50. Scholz J, Woolf CJ. The neuropathic pain triad: neurons, immune cells and glia. Nature neuroscience. 2007 Nov; 10(11):1361–8.
51. Thacker MA, Clark AK, Marchand F, McMahon SB. Pathophysiology of peripheral neuropathic pain: immune cells and molecules. Anesthesia and analgesia. 2007 Sep; 105(3):838–47. [PubMed: 17717248]

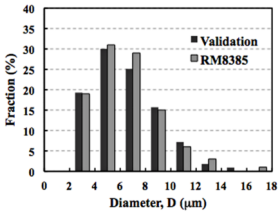

Figure 1.
Histogram of the particle size from a validation sample as compared to the NIST reference standard (RM8385). The mean % difference (± sem) across all size ranges was 1.3 ± 0.4.

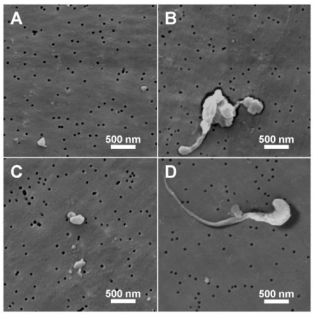

Figure 2.
Representative ESEM images of UHMWPE wear debris from (**A,B**) TDR and (**C,D**) THA cohorts. (magnification 12,000×).

Figure 3.
Histogram of the **A**) equivalent circular diameter, **B**) aspect ratio, and **C**) roundness of TDR and THA UHMWPE wear debris. Bars represent the mean percentage of particles within each size/shape range (± sem).

Table 1

Comparison of the 5 non-coated single-level TDRs included in the present study and the 11 cases from the original study of the first 16 patients[32] (± standard error of the mean).

	5 non-coated single TDRs (included)	**Residual 11 TDR cases from the original cohort[32] (excluded)**	***p*-value**
Age at implantation (year)	39.6 ± 2.8	42.0 ± 2.1	0.61
Gender ♀-♂	3 – 2	9 – 2	0.37
Implantation time (years)	9.2 ± 1.0	7.5 ± 1.3	0.25
Mean number of UHMWPE particles/mm^2 (≥ 2.05 μm)	114.0 ± 52.8	280.0 ± 100.8	0.78
Macrophages (Mirra classification 0 - 1$^+$ - 2$^+$ - 3$^+$)	0 – 1 – 3 – 1	2 – 0 – 4 – 5	0.54
Giant-cells (Mirra classification 0 - 1$^+$ - 2$^+$ - 3$^+$)	2 – 2 – 0 – 1	4 – 1 – 4 – 2	0.60

Table 2

Summary of patient and clinical variables for TDRs and THRs.

Implant number	Sex	Age at implantation	Prosthesis	Revision reason	Implantation time (years)	Air/inert	Level	Endplate size
TDR								
Maa003	M	46	Charité (LINK)	Subsidence, back and leg pain	6	Unknown	L4-5	3
Maa009	M	39	Charité (LINK)	Pain due to severe facet joint degeneration L4/L5 and degeneration disc L1-L2 and L3-L4	10	Air	L4-5	3
Maa010	F	34	Charité (LINK)	Persisting pain after failed posterior fusion	8	Unknown	L5-S1	3
Maa013	F	33	Charité (LINK)	Instability/Retrolisthesis L1-L2/L2-L3; Pseudo-arthrosis L4-L5; Anterior position & possible wear L3/L4	12	Air	L3-4	2
Maa018	F	33	Charité (LINK)	Persistent lumbar pain and right leg pain; disc degeneration L3/L4	10	Air	L4-5	3
THA								
CWH002	M	67	Zimmer HGPII	Polyethylene wear, Osteolysis	13	Air	n/a	n/a
RIH120	F	62	Biomet Hexloc	Polyethylene wear, Osteolysis	15	Air	n/a	n/a
RIH426	F	43	Biomet Hexloc	Polyethylene wear, Osteolysis	14	Air	n/a	n/a
RIH134	M	Unknown	Biomet Hexloc	Polyethylene wear, Loosening (Femoral)	11	Air	n/a	n/a
RIH369	F	45	Biomet Hexloc	Polyethylene wear, Loosening (Acetabular)	13	Air	n/a	n/a
p-value	1.00	0.05			0.02			

Abbreviations: L, lumbar vertebrae; HGP, Harris-Galante Porous

Table 3

Summary of wear particle characteristics

Parameter	Equation	Definition
ECD *(μm)*	$2*\sqrt{(A/\pi)}$	Diameter of a circle with an area equivalent to the particle area (A)[34]
AR *(unitless)*	d_{max}/d_{min}	Ratio of major (d_{max}) to minor diameter (d_{min})[34]
R *(unitless)*	$(4*A)/(\pi*d_{max}^2)$	Measure of circularity varying from zero to one (perfect circle) [34]

Abbreviations: ECD, equivalent circular diameter; AR, aspect ratio; R, roundness; A, particle area.

Table 4

Summary of UHMWPE particle concentration, size and shape in TDR and THA.

Implant number	Tissue weight (gram)	Number of particles ($\times 10^9$/gram)	Particles per year ($\times 10^9$/gram/yr)	ECD mean ± sem, median	Aspect ratio mean ± sem, median	Roundness mean ± sem, median
TDR						
Maa003	0.0267	1.794	0.287	0.481 ± 0.004, 0.376	2.062 ± 0.011, 1.864	0.536 ± 0.002, 0.536
Maa009	0.0238	1.488	0.146	0.476 ± 0.007, 0.360	1.870 ± 0.013, 1.709	0.579 ± 0.003, 0.585
Maa010	0.0223	1.990	0.235	0.334 ± 0.012, 0.266	1.848 ± 0.024, 1.652	0.590 ± 0.006, 0.605
Maa013	0.0224	1.523	0.119	0.633 ± 0.007, 0.521	1.859 ± 0.011, 1.670	0.585 ± 0.003, 0.599
Maa018	0.0207	1.308	0.124	0.396 ± 0.009, 0.299	1.809 ± 0.018, 1.647	0.601 ± 0.004, 0.607
Mean ± sem		**1.621 ± 0.121**	**0.182 ± 0.034**	**0.464 ± 0.050**	**1.890 ± 0.044**	**0.578 ± 0.011**
THA						
CWH002	0.0252	2.262	0.173	0.618 ± 0.009, 0.376	1.903 ± 0.009, 1.736	0.570 ± 0.002, 0.576
RIH120	0.0246	2.481	0.159	0.701 ± 0.004, 0.564	2.002 ± 0.007, 1.791	0.552 ± 0.001, 0.558
RIH426	0.0240	3.237	0.294	0.468 ± 0.002, 0.399	1.785 ± 0.005, 1.678	0.594 ± 0.001, 0.596
RIH134	0.0263	1.798	0.127	0.407 ± 0.005, 0.307	2.039 ± 0.015, 1.791	0.553 ± 0.003, 0.558
RIH369	0.0246	1.881	0.145	0.454 ± 0.011, 0.344	2.207 ± 0.037, 1.810	0.551 ± 0.006, 0.555
Mean ± sem		**2.332 ± 0.258**	**0.180 ± 0.030**	**0.529 ± 0.055**	**1.987 ± 0.070**	**0.564 ± 0.008**
p-values		0.03	0.60	0.60	0.35	0.35

Abbreviations: ECD, equivalent circular diameter; sem, standard error of the mean.

Table 5

Summary of Visible Damage on the UHMWPE Core

Implant number	Dome penetration (mm)	Dome penetration rate (mm/yr)	Rim penetration (mm)	Rim penetration rate (mm/yr)
Maa003	0.1080	0.0173	0.418	0.0669
Maa009	0.5410	0.0529	0.085	0.0083
Maa010	0.3706	0.0437	0.019	0.0022
Maa013	0.3572	0.0280	0.103	0.0080
Maa018	0.3332	0.0314	0.059	0.0055
Mean (± sem)	**0.3420 ± 0.0691**	**0.0347± 0.0062**	**0.1368 ± 0.0717**	**0.0182 ± 0.012**

Abbreviations: mm, millimeter